CHEMICAL ENGINEERING TRANSACTIONS
VOL. 69, 2018
A publication of AIDIC
The Italian Association of Chemical Engineering
Online at www.aidic.it/cet
Guest Editors: Elisabetta Brunazzi, Eva Sorensen

ISBN 978-88-95608-66-2; **ISSN** 2283-9216
DOI: 10.3303/CET1869126

In-line Analysis of Entrainment through Image based Probe Measurement Technology

Jonas Schulz*, Hans-Jörg Bart

Chair of Separation Science and Technology, University of Kaiserslautern, Germany
bart@mv.uni-kl.de

A new optical approach for entrainment detection is presented using a measurement probe, which is applicable at different axial and radial positions within the column in an industrial environment. The new developed probe enables in-line detection and on-line analysis of entrained droplets between separation stages respectively at the column head. Different test rigs (up to DN 450) are used for data sampling. The new construction of the probe uses a purge gas stream to protect the front window of the probe from wetting, providing a non-wetted and clear view, leading to better image qualities and low purge medium consumption. A comparison of the measurement results with the Phase-Doppler-Anemometry shows a good agreement. As expected, entrainment depends on liquid and gaseous flow rates. Capability of models from literature to cope with the available data are discussed.

1. Introduction

Counter flow distillation and absorption columns feature a distinct operating range, in which the columns perform the separation process with high efficiency. Outside this range, entrainment, blowing, choking and weeping diminish the performance of the separation. Furthermore, the aforementioned conditions constitute a serious threat to column internals and plant equipment (Staak, 2010). Entrainment describes the recycling of liquid from lower to upper trays respectively from the last tray in the top product line and diminishes efficiency (Kister & Haas, 1988). In addition, already Colburn (1936) recognizes that a precise estimation of entrainment enables the design of more compact distillation systems resulting in lower investment costs. In context of this contribution, a new approach to investigate entrainment is capable of detecting entrained droplets on a photographic image basis within a cold flow distillation system, applying a modified version of the previously presented Optical Multimode Online Probe (OMOP) (Mickler & Bart, 2013; Mickler et al., 2013). Experiments refer to two different cold flow test rigs. A DN 200 absorption system generates droplets with aid of a nozzle and serves as a test rig for validation purposes by a comparison between the measurement results of the modified OMOP and the Phase-Doppler-Anemometry. A DN 450 rectification system generates droplets with aid of a sieve tray. Additionally, a capture tray for entrainment quantification (Puppich & Goedecke, 1987) enables the comparison with results of the modified OMOP. This comparison is helpful to deepen the understanding of the complex behaviour of entrainment.

2. Theoretical Background

Souders & Brown (1934) establish a force balance between gravitational and buoyancy force acting on a droplet based on considerations of Villamil (1917).

$$\frac{\pi g d^3}{6}\left(\rho_l - \rho_g\right) = \frac{k\rho_l \pi d^2}{4} v^2 \tag{1}$$

Concerning this equilibrium, the variable d represents the diameter of the droplet, while ρ_l and ρ_g sum up for the densities of the liquid and gaseous phase respectively.The velocity of the surrounding medium to hold a droplet in suspension is defined as.

Please cite this article as: Schulz J., Bart H.J., 2018, In-line analysis of entrainment through image based probe measurement technology, Chemical Engineering Transactions, 69, 751-756 DOI: 10.3303/CET1869126

$$v = \sqrt{\frac{2gd}{3k}} \cdot \left(\frac{\rho_l - \rho_g}{\rho_g}\right)^{1/2} \quad (2)$$

Based on this consideration, a critical flow factor $F_{crit} = v \cdot \sqrt{\rho_l}$, can predict where a droplet is just floating before being entrained. For a rough assessment of tray capacity E_{cap}, entrainment is defined as the ratio of entrained liquid flow $\dot{L}'$ to vapor flow $\dot{V}$. The ratio E_{eff} of entrained liquid flow to liquid flow across the tray $\dot{L}$ gives information about the tray efficiency (Uys et al., 2012)

$$E_{cap} = \frac{\dot{L}'}{\dot{V}} \quad (3)$$

$$E_{eff} = \frac{\dot{L}'}{\dot{L}} \quad (4)$$

Entrained liquid E_{eff} up to 5 % (Kister & Haas, 1988) is often tolerated, but becomes critical at high volatility separations, where liquid concentrations between trays vary significantly. The easiest way to quantify entrainment is achieved with a capture tray (Puppich & Goedecke, 1987). Advantages of applying a capture tray and demister are the integral quantification of the entrained liquid and the simple reconstruction of the column. However, the transferability of results from an experimental setup with a capture tray to a column in industrial scale is limited, not least because a random quantity of droplets falls back by hitting the tray bottom. Consequently, Kister & Haas (1987) underline, that correlations originating from laboratory and pilot scale experiments possess a limited range of validity.

Another approach is the investigation of entrainment between trays directly inside the column. Experiments only require a measurement access and can even take place in industrial scale columns. For example, the Phase-Doppler-Anemometry (PDA) is capable of detecting and analyzing droplets precisely in terms of size, velocity and hold-up. Measurements with PDA are non-invasive and require an access for instance via a transparent window. A major disadvantage of this instrument is the limited industrial applicability due to high calibration and measurement efforts, spatial and local requirements of the measurement access and specific instruction and way of working in respect of safety and explosion-proof (Bauckhage, 1996; Lichti & Bart, 2017). Successful detections of droplets in liquid/liquid systems (Amokrane et al., 2016; Maß et al., 2012; Mickler & Bart, 2013) and bubbles in gaseous/liquid systems (Panckow et al., 2013) identify imaging methods as an alternative option for entrainment detection in liquid/gaseous systems. In general, imaging methods are flexible in respect of application and measurement access. Measurement systems based on transmitted light and telecentric optics require two measurement access points placed diametrically to each other. The positioning of camera unit and light source generates shadowgraphic images with highest contrasts, which facilitates the subsequent image evaluation including low calibration and measurement efforts (Bart et al. 2011, Lichti & Bart, 2017). For large diameter columns an endoscopic shadowgraphic probe was developed, which can be operated using an existing nozzle at the column shell (Lichti et al. 2015).

3. Material

3.1 Applied measurement instruments

The modified OMOP represents a constructive enhancement of the original OMOP first introduced by Mickler & Bart (2013). The probe is suitable for the measurement of dispersed liquids in a gaseous phase. The modified OMOP is capable of preventing entrained droplets coalescing at the inspection window with aid of a pneumatic purging system, as wipers likewise in a car are not applicable. A transmitted light technique allows generating high-contrast images of entrained droplets. A telecentric lense enables a distance independent imaging of droplets within the measurement area. An integral coverage of the inner column diameter is achieved by a measurement section, which contains accesses on different heights and allows a radial adjustment of the probe within the column (from wall to middle). The PDA constitutes an established measurement method (Bauckhage, 1996), which is suitable for a comparison with the modified OMOP in an air-water system.

3.2 Pilot scale test rig

The pilot scale test rig consists of a DN 200 glass column (De Dietrich Process Systems GmbH), with gaseous feed entrance at the column bottom and a full cone injection nozzle (Lechler GmbH) at the center of the column body. The column top contains a wire mesh separator (Raschig GmbH). A measurement section for the modified OMOP and PDA is implemented below the separator respectively above the nozzle. The second

test rig consists of a DN 450 glass column (DE Dietrich Process Systems GmbH), with gaseous feed entrance at the column bottom and liquid feed entrance at the column top. The column can be equipped with a maximum of three trays (sieve and fixed valve; spacing 500 mm) to guarantee a homogeneous flow or 1.5 m of structured (RMP S250) or random packings (Pall Rings). Experiments conducted for this contribution were executed with two sieve trays (d_h= 11 mm; h_{weir} = 50 mm; A_{active} = 0.139 m^2). One measurement section above the last separation stage allows measurements with the modified OMOP and PDA from TSI (Innova 70C series ion laser) at different axial and radial positions. The aforementioned capture tray (Raschig GmbH) represents the column top and allows an exact quantification of the entrained liquid. Both test rigs are cold flow systems running with unsaturated air and water. *Figure 1* represents a basic outline of the DN 450 test rig.

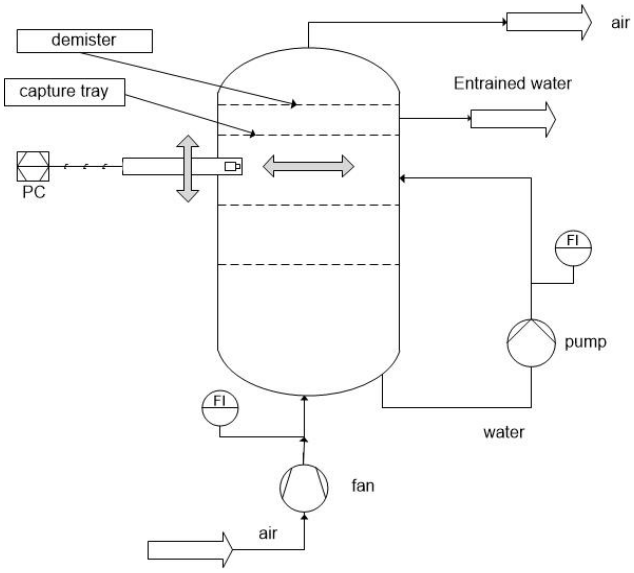

Figure 1: Basic illustration of the DN 450 test rig equipped with two trays plus capture tray and demister

4. Experimental Results

4.1 Comparison of modified OMOP with PDA in DN 200 test rig

The comparison between both measurement methods given in *Figure 2* is performed with the aforementioned nozzle at a liquid flow rate of 0.36 L/min. The graph shows a strong accordance between both measurement methods. The PDA tends to detect a higher amount of smaller droplets in a range of 5 to 40 μm, while the modified OMOP detects larger droplet sizes on a range of 100 to 260 μm. Both measurement methods identify droplets with a size of 60 μm as the most prevalent droplet size at this volumetric flow rate.

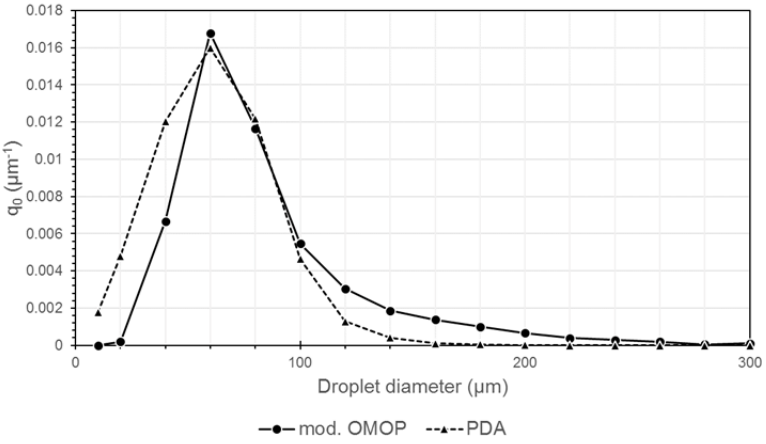

Figure 2: Comparison of PDA and modified OMOP measurements results at 0.36 L/min H_2O flow

4.2 Entrainment measurements with capture tray and modified OMOP in DN 450 test rig

Measurements in the DN 450 test rig were performed with H_2O loads up to 2.92 $\mathrm{m^3/hm}$ and gaseous loads up to F-Factor 2.5 $\sqrt{Pa}$ with the aforementioned sieve tray. *Figure 3* depicts the entrainment rates quantified by capture tray and demister (E_{eff}). The graph shows a negative effect of the H_2O load on entrainment. The amount of entrained liquid decreases by increasing H_2O loads, which is in line with results of Kister & Haas (1987, 1988). According to Staak (2010) this behavior is reasonable, as a higher amount of liquid on the tray results in a broader energy dissipation of the gaseous flow. Consequently, droplets erupting out of the liquid phase hold less kinetic energy and will less often reach the next tray. An additional explanation could be an enhanced coalescence to bigger droplets being more difficult to entrain. *Figure 3* also reveals a strong dependence of entrainment rates on gaseous loads, which corresponds to the findings of many authors (Fair, 1961; Souders & Brown, 1934; Stichlmair, 1977). In this case, the gaseous flow accelerates the droplets erupting out of the liquid much stronger. Accordingly, these droplets will more likely reach the next tray leading to higher entrainment.

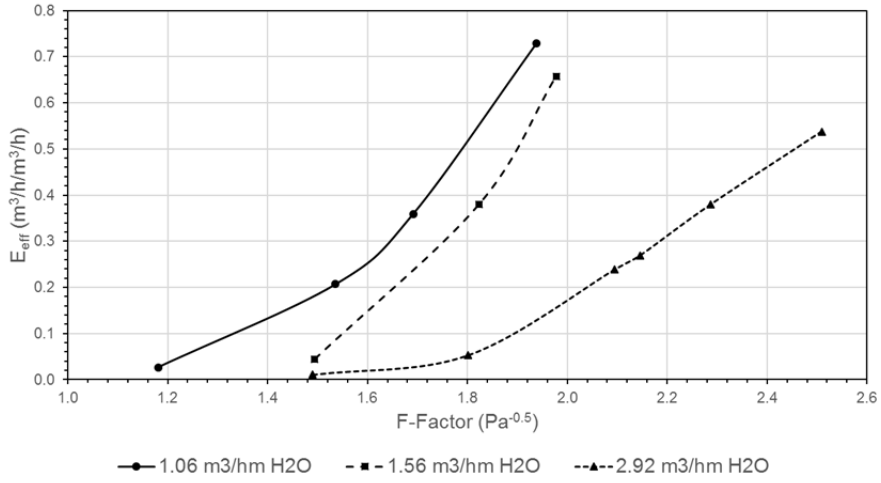

Figure 3: Entrainment rates $\dot{E}_{eff}$ for three different H_2O loads versus F-factor

In contrast to entrainment data from literature the modified OMOP allows a quantification of the droplet size distributions of entrained liquid at different gaseous and liquid flow rates. Measurement height is set to 247.5 mm above the upper sieve tray. Therefore, a distance of 252.5 mm between capture tray and modified OMOP remains, which implies that optical measurements may contain rising and falling droplets leading to a detection of entrained and re-entrained liquid. The following droplet size distributions depicted in *Figure 4* at an H_2O load of 1.06 $\mathrm{m^3/hm}$ and gaseous loads up to 1.94 $\sqrt{Pa}$ show a clear dependence on gaseous loads.

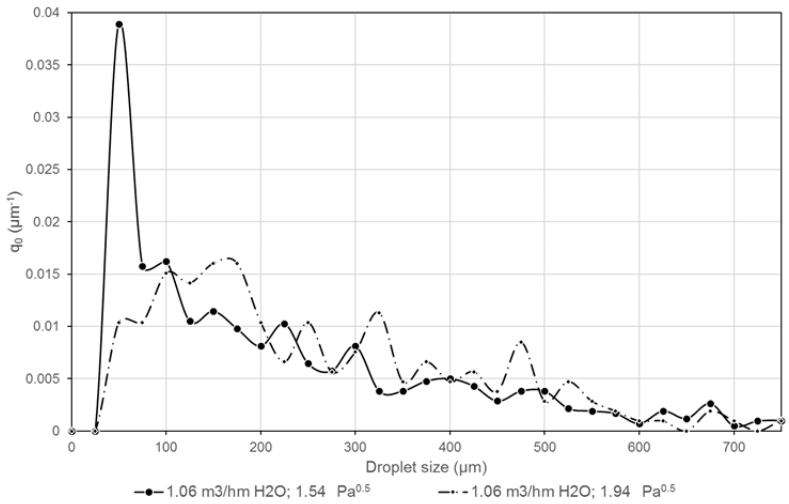

Figure 4: Droplet size distributions of entrainment captured with modified OMOP at 1.54 and 1.94 $\sqrt{Pa}$

The graph for 1.54 $\sqrt{Pa}$ gaseous load shows a peak at 50 μm and usually holds droplets larger than 100 μm less often than the graph for 1.94 $\sqrt{Pa}$. On the other hand, the droplet size distribution detected at 1.94 $\sqrt{Pa}$ shows a most frequent droplet size of 175 μm and in most cases a higher frequency for all droplet sizes larger than 100 μm. Theoretical considerations of equation 1 & 2 predict that droplet sizes increase with an increase of the gaseous flow rate, due to the higher lift force of the gaseous flow. This assumption is fulfilled, as the most frequent droplet size is 100 μm larger at 1.94 $\sqrt{Pa}$. A calculation of the critical flow factor based on equation 2 gives $F_{crit,1}$ = 1.64 $\sqrt{Pa}$ for a droplet size of 175 µm for the experiment with 1.94 $\sqrt{Pa}$. Consequently, a F-factor above 1.62 $\sqrt{Pa}$ will most likely entrain droplets larger than 175 µm. The critical flow factor for the graph with 1.54 $\sqrt{Pa}$ gaseous load is $F_{crit,2}$ = 0.88 $\sqrt{Pa}$ for 50 μm droplets. Higher gas velocities will entrain more droplets larger than 50 μm, which is clearly recognizable by comparing both graphs.
According to the droplet size distributions depicted in Figure 5, at H_2O loads up to 2.92 $\mathrm{m^3/hm}$ and gaseous loads of approximately 1.5 $\sqrt{\mathrm{Pa}}$ droplet sizes appear to increase with increasing H_2O loads. Equations 1 & 2 suggest constant droplet sizes at equal gaseous loads and are therefore not suitable to explain this behavior. There are three possible explanations for this contradiction. At first, the three graphs show a gas velocity difference of only 0.07 $\sqrt{Pa}$, which suggests no distinct change in droplet size. This is at least correct for the most frequent droplet size of 50 μm. Secondly, an increase of H_2O load up to 2.92 $\mathrm{m^3/hm}$ reduces the effective tray spacing well below the mechanical spacing of 500 mm due to the higher liquid level on the sieve tray. Consequently, detected droplets at a fixed measurement height are larger per se, due to the reduced distance between liquid surface and the measurement position. In the third place, an increase of the H_2O load will most likely enhance coalescence of single droplets. Also Staak (2010) underlines that entrained liquid becomes more likely apparent in the form of agglomerates than small droplets, if liquid loads are increased at constant gaseous loads.

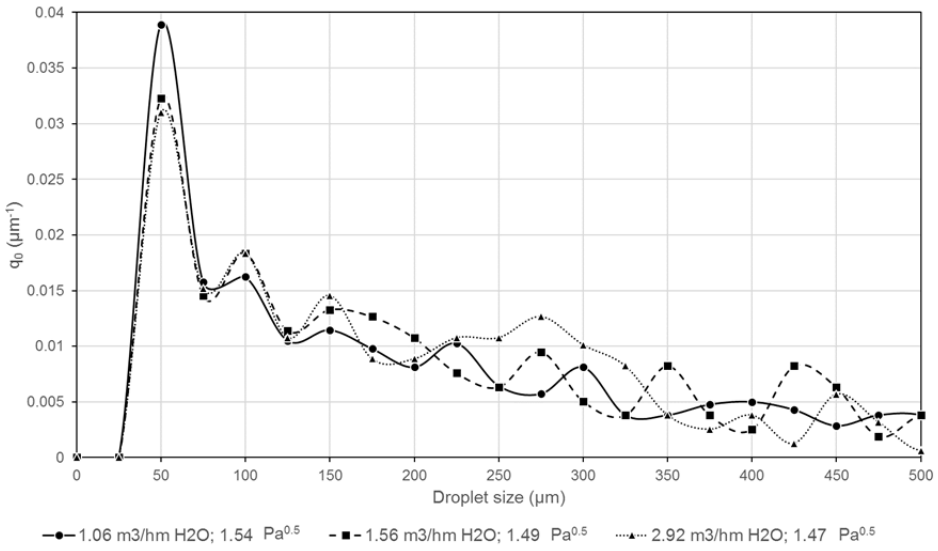

Figure 5: Droplet size distributions of entrainment captured with modified OMOP up to 2.92 m^3/hm

5. Conclusions & Outlook

Measurement results captured with the modified OMOP show a good agreement with the established PDA measurement method. Experiments conducted in the DN 450 test rig with a wire mesh separator and a capture tray, show as expected high entrainment rates at high gaseous loads and low entrainment rates at high H_2O loads, which corresponds to the results of Kister & Haas (1987, 1988). Droplet size distributions at higher gaseous loads show as theoretically expected larger droplet sizes due to the higher lift force of the gaseous phase. Droplet size distributions at constant gaseous loads but multiple liquid loads partly confirm the force balance model of Souders & Brown (1934). The most frequent droplet size remains constant at 50 μm, due to an almost constant gas velocity. On the other hand, higher liquid loads generate larger droplets in an area between 100 μm and 500 μm, probably due to a reduced tray spacing caused by a higher liquid level on the tray. Another explanation may be an enhanced coalescence to larger droplets due to the increased amount of liquid flowing over the tray.

Acknowledgments

We wish to thank the German Federal Ministry for Economic Affairs and Energy for their financial support and our partners in the joint project TERESA.

References

Amokrane, A., Maaß, S., Lamadie, F., Puel, F., Charton, S., 2016, On droplets size distribution in a pulsed column. Part I: In-situ measurements and corresponding CFD–PBE simulations, Chemical Engineering Journal, 296, 366–376.

Banerjee, T.S., Roy, N.K., Rao, M.N., 1969, Studies on entrainment of drops in flow through orifices: Part II Magnitude of entrainment from liquids, Indian Journal of Technology, 7, 308–311.

Bart, H.-J., Mickler, M., Jildeh: H.B., 2012, Optical Image Analysis and Determination of Dispersed Multi Phase Flow for Simulation and Control, Chapter I, in: Optical Imaging: Technology, Methods & Applications, Akira Tanaka and Botan Nakamura (eds.), 1-63, Nova Science, N.Y. Lancaster, 2012.

Bauckhage, K., 1996, Gleichzeitige Erfassung von Partikelmerkmalen und Eigenschaften mehrphasiger Strömungen mit Hilfe der Phasen-Doppler-Anemometrie, Chemie Ingenieur Technik, 68, 253–266.

Bennett, D.L., Kao, A.S., Wong, L.W., 1995, A mechanistic analysis of sieve tray froth height and entrainment. American Institute of Chemical Engineers Journal, 41, 2067–2082.

Fair, J., 1961, How to Predict Sieve Tray Entrainment and Flooding, Petroleum Management, 33, 211–218.

Humphrey, J.L., 1995, Separation Processes: Playing a critical role, Chemical Engineering Progress, 31–39.

Hunt, C.D.'A., Hanson, D.N., Wilke, C.R., 1955, Capacity factors in the performance of perforated-plate columns, American Institute of Chemical Engineers Journal, 1, 441–451.

Kister, H.Z., Haas, J.R., 1987, Sieve tray entrainment prediction in the spray regime. A Three-day Symposium Organised by the Institution of Chemical Engineers Fluid Separation Group and the EFCE Distillation, Absorption and Extraction Working Party, 07.09.1987-09.09.1987, Brighton Centre, Brighton, England. Institution of Chemical Engineers.

Kister, H.Z., Haas, J.R., 1988, Entrainment from sieve trays in the froth regime. Ind. Eng. Chem. Res., 27, 2331–2341.

Koziol, A., Mackowiak, J., 1990, Liquid Entrainment in Tray Columns. Chemical Engineering and Processing: Process Intensification, 27 (3), 145–153.

Lichti, M., Bart, H.-J., Roth, C., Vorrichtung für Bildaufnahmen eines Messvolumens in einem Behälter, EU Pat 10 2015 103 497.2, 10.3.2015.

Lichti, M., Bart, H.-J., 2017, Partikelmesstechnik in der Fluidverfahrenstechnik, Chemie Ingenieur Technik, 89, 1599-1610.

Maaß, S., Rojahn, J., Hänsch, R., Kraume, M. (2012) Automated drop detection using image analysis for online particle size monitoring in multiphase systems, Computers & Chemical Engineering, 45, 27–37.

Mickler, M., Bart, H.-J., 2013, Optical Multimode Online Probe: Erfassung und Analyse von Partikelkollektiven, Chemie Ingenieur Technik, 85, 901–906.

Mickler, M., Boecker, B., Bart, H.-J., 2013, Drop swarm analysis in dispersions with incident-light and transmitted-light illumination, Flow Measurement and Instrumentation, 30, 81–89.

Panckow, R., Maaß, S., Emmerich, J., Kraume, M., 2013, Automatisierte Quantifizierung von Blasengrößenverteilungen in einem gerührten Luft/Wasser-System, Chemie Ingenieur Technik, 85, 1036–1045.

Puppich, P., Goedecke, R., 1987, Investigation of entrainment in tray columns. Chemical Engineering and Technology, 10, 224–230.

Staak, D., 2010, Absicherung von Destillationskolonnen im nicht bestimmungsgemäßen Bereich, PhD Thesis, Technische Universität Berlin, Berlin, Germany.

Souders, M., Brown, G.G., 1934, Design of Fractionating Columns: I. Entrainment and Capacity, Industrial and Engineering Chemistry, 26, 98–103.

Stichlmair, J., Hofer, H., 1978, Mitreißen von Flüssigkeit aus der Zweiphasenschicht von Kolonnenböden, Chemie Ingenieur Technik, 50, 553.

Stichlmair, J., Mersmann, A., 1977, Dimensionierung von Bodenkolonnen für die Absorption und Rektifikation, Chemie Ingenieur Technik, 49, 106–117.

Uys, E.C., Schwarz, C.E., Burger, A.J., Knoetze, J.H., 2012, New froth behaviour observations and comparison of experimental sieve tray entrainment data with existing correlations, Chemical Engineering Research and Design, 90, 2072–2085.

Villamil, R. de, 1917, Resistance of air, E. & F.N. Spon Ltd., 57 Haymarket, S.W., London.